NASA TECHNICAL NOTE

NASA TN D-3061

NASA TN D-3061

AN INVESTIGATION OF A DEFORMING ENERGY-ABSORPTION SYSTEM FOR SPACE-VEHICLE LANDINGS

by Robert W. Warner, Robert M. Sorenson, and Arthur J. Kaskey

Ames Research Center
Moffett Field, Calif.

NATIONAL AERONAUTICS AND SPACE ADMINISTRATION • WASHINGTON, D. C. • OCTOBER 1965

NASA TN D-3061

AN INVESTIGATION OF A DEFORMING ENERGY-ABSORPTION SYSTEM FOR SPACE-VEHICLE LANDINGS

By Robert W. Warner, Robert M. Sorenson,
and Arthur J. Kaskey

Ames Research Center
Moffett Field, Calif.

NATIONAL AERONAUTICS AND SPACE ADMINISTRATION

For sale by the Clearinghouse for Federal Scientific and Technical Information
Springfield, Virginia 22151 – Price $2.00

AN INVESTIGATION OF A DEFORMING ENERGY-ABSORPTION SYSTEM FOR SPACE-VEHICLE LANDINGS

By Robert W. Warner, Robert M. Sorenson,
and Arthur J. Kaskey
Ames Research Center

SUMMARY

A deforming system for protecting a space vehicle during a landing impact is described and experimentally evaluated. The impact energy is absorbed mostly by the cutting of plastic foam pads, but partially by the buckling of their tubular support structure. Expandable foam is chosen because of its advantages in packaging and in reducing penetration of the landing surface. The foam and its supporting structure are utilized in such a way as to benefit tip-over stability and over-all efficiency of energy absorption (energy absorbed divided by the weight of the entire energy absorbing system), with priority given to the latter. The resulting system, when compared with another proposed system, has exceptionally good over-all efficiency, namely, 545 ft-lb/lb, but has less satisfactory stability, with the model vehicle restricted to a 5° ground slope and nearly vertical impacts.

INTRODUCTION

Landing has always been one of the most dangerous aspects of flight, and a so-called soft space-flight landing will probably be no exception. Landing problems will include energy absorption, deceleration loads, and vehicle tip-over because a space vehicle is likely to land with a substantial velocity on a rough, slanted surface. A large velocity will obviously have to be tolerated at touchdown for parachute landings on planets. Even a vehicle capable of hovering near the landing surface may experience a significant impact if the rocket engines fail, or have to be turned off prematurely to prevent the exhaust from disfiguring the landing area. In addition, a certain amount of control error is expected during the landing phase. For these reasons, it is generally accepted that energy absorbing systems will be used for so-called "soft" landings of space vehicles (refs. 1 and 2).

Because a space-landing system will generally be used only once, a controlled failure of the system can be utilized. The simplicity and resulting reliability of a failure system are particularly appropriate for the large temperature gradients and hard vacuum of the space environment.

Space-landing systems have already received considerable attention, as indicated in references 3 to 33. In the present paper, attention will be restricted to a particular system. In contrast to references 3 to 33, the choice of materials for the present system is based primarily on certain

requirements (called "supplementary" herein) other than tip-over stability and a high over-all efficiency of energy absorption. The supplementary requirements are related to packaging, penetration of the landing surface, and a stable blast-off configuration. The primary purpose of the present paper is to show, experimentally, what can be done on tip-over and over-all efficiency with a restricted amount of development of such a system. It is intended, thereby, to provide information on the feasibility of incorporating the present "supplementary" requirements in a final design choice.

The "supplementary" requirements considered herein are described first. Then the model vehicle based largely on those requirements is detailed, together with the apparatus and test technique for evaluating the model. The manner in which the model was developed is described next, followed by results on efficiency and tip-over stability.

The model vehicle description and part of the results given herein have been presented briefly in reference 33 as one means of considering needed materials improvements for space-landing systems. In the present paper, the issue of materials improvements is not emphasized; and the model description and results are much more complete than in reference 33. With respect to hard-surface and nonvertical landings, the present results have not been published elsewhere.

NOTATION

V vertical component of impact velocity, ft/sec

α ground slope, deg

β impact flight-path angle above the horizontal, deg

η over-all efficiency of energy absorption (energy absorbed divided by the total weight of the energy absorbing system), ft-lb/lb

η_M foam mechanism efficiency (energy absorbed by the foam divided by the weight of the foam), ft-lb/lb

METHODS, RESULTS, AND DISCUSSION

Requirements for Landing System

An energy absorbing system should be required to absorb a specified impact energy with high over-all efficiency, η, within a certain acceleration limit, and to prevent the vehicle from tipping over as a result of unsymmetrical landing conditions. These are the two basic requirements. For the present, however, attention is restricted to the following supplementary requirements: The landing system should

(1) Occupy a small packaging volume
(2) Prevent excessive penetration of the landing surface
(3) Provide a stable firing platform for return blast-off

Requirement (1) suggests the consideration of plastic foam as the primary energy absorber since it should be foamable in flight after earth exit. This would result in a low volume of material in the energy absorbing system during earth exit. An efficient distribution of such a small volume would then require a minimum of fairing material for passage through the atmosphere. This could result in a significant weight saving. (It should be noted that polystyrene foam was used in the present experiments, rather than the more easily foamable polyurethane, only because a suitable polystyrene happened to be more readily available.)

Requirement (2) derives from the controversy over the depth of low strength lunar crust (as in refs. 34-48). Since future unmanned probes may leave the controversy unresolved, it would seem necessary to accommodate requirement (2) as far as possible within weight limitations. Plastic foam does this excellently because it permits a long sinking stroke and a large bearing area without causing a major packaging problem. Both a long stroke and a large bearing area tend to reduce the chance of penetrating the lunar crust to such a depth as to hamper the exploration of the surface or the return blast-off. Requirements (1) and (2) have led to the choice of plastic foam to absorb most of the prescribed impact energy in the present example.

The third requirement has led to the consideration of a three-legged landing system. With such a system, no mechanical cranking of the legs is required to provide blast-off stability after landing.

Model, Apparatus, and Experimental Technique

A model of an energy absorbing system based largely on the above supplementary requirements is shown in figure 1. This is the final version evolved from a series of tests and studies and is shown undeformed. Three ski-pole type cutters rest on three hollowed-out pieces of polystyrene foam, and the cutting of the foam absorbs the largest part of the impact energy. The welded, tubular, compression members fail near the end of the foam cutting stroke to absorb additional energy in buckling. These members are curved to assure consistent upward buckling.

Figure 2 shows a complete model for vertical impact after a landing in which both the cutting and the buckling have taken place. The nearly solid wooden body of the model contains no fluid, so the potentially important effect of fuel sloshing on tip-over stability is not evaluated. The weight of the model body, including the fins, which provide stability during the vertical drops, is 33.4 pounds. The weight of the energy absorbing system, including everything below the thrust ring, is 1.68 pounds, or 4.8 percent of the combined model body and landing system weight.

A picture of a model for nonvertical impact prior to release is shown in figure 3. The model is identical to that of figure 2, except that the fins

have been removed and runners have been added on either side of the model. The runners permit the model to slide down the rails shown in figure 3. The model weight, center-of-gravity location, and moment of inertia are identical for vertical and nonvertical impacts. Numerical values for these and other model parameters are given in figure 4.

The model body, with its finned or unfinned nose boom, cannot be regarded as a scaled model of any prototype vehicle. At a scaling of roughly 10 to 1, however, it can be considered as crudely representative of the Lunar Excursion Module, or LEM, class (see appendix A for scaling).

A portion of the experimental apparatus and facility is shown in each of figures 1, 2, and 3. In figure 1, three piezoelectric accelerometers are shown at right angles to each other. In actual operation, the accelerometers are connected to their amplification and read-out systems by coaxial cables 150 feet long.

The test facility for vertical impacts is shown in figure 2. The backboard is lined to measure impact velocities with the aid of high-speed motion pictures. The dust on which the model rests in figure 2 is a 1-1/2-inch-thick layer of crushed basalt. (For sieve results on the basalt, given by the supplier and the U. S. Geological Survey, see fig. 5.) The platform which holds the dust can be set at various ground slopes although it is shown horizontal. For a smooth, hard surface, a heavy steel sheet, 0.12 inch thick, is placed on top of the dust.

The platform in figure 3 is identical to that in figure 2. The facility in figure 3 is adapted to nonvertical impacts by the slanted rails which are 30 feet long. The stripes on the rails, together with high-speed motion pictures and the pointer attached to the model, serve to measure resultant velocity. The model attitude is essentially vertical at impact, and its pitch rate essentially zero. Additional details on the apparatus and facility, together with a discussion of various measurement errors, are given in appendix B.

Much of the experimental technique is suggested by figures 2 and 3. When the basalt dust surface is used, the surface is prepared by disturbing the dust and then loosely striking it off level. This ensures a repeatable surface. (In fig. 3, the surface has not yet been prepared.)

For the vertical impacts, the test technique is simply to hoist the model of figure 2 by means of a rope attached to an overhead elevator. When the model has been oriented with one pad pointing directly uphill or downhill, the rope is cut. If the model tips over or the accelerometers read higher than a specified limit, the ground slope or the drop height is lowered for the next drop. Otherwise, the slope or height is raised until the boundary on acceleration and tip-over is reached.

For the nonvertical impacts, the rails in figure 3 are set at a given angle to establish a given flight path. Then the landing platform height is adjusted so that the first foam to hit the landing surface is 1 inch above the surface when the model runners leave the rails. The model is then pulled a

certain distance up the rails by a rope pulley and released by cutting the rope. The distance up the rails and the surface slope are varied to establish the same type of boundary found for the vertical impacts. In contrast to figure 3, the rope is generally in the plane of the model runners, and this plane contains the model center of gravity.

Development Procedure

It has been pointed out that the plastic foam material and the three-legged configuration were selected because of the supplementary requirements listed earlier. After these selections were made, however, a development program was initiated to achieve a high over-all efficiency of energy absorption, η, and at least a fair degree of tip-over stability.

Because it is more difficult to control vertical velocity than horizontal velocity in a vacuum environment with a strong gravity field, greater priority was given to a high η for vertically symmetrical landings than to good stability for unsymmetrical landings. Hence, in contrast to many of the models in references 3 to 33, the frame supporting the primary energy absorber (foam, in the present case) was located entirely below the model body, as seen in figures 1 to 3; and the outreach of the frame beyond the body perimeter was relatively low. The low outreach tended to improve η by limiting the frame weight. The location of the frame below the body, rather than alongside it, permitted the compression members to be designed for a long buckling stroke after the foam stroke is nearly completed. The buckling benefited η partly by increasing the energy absorption but mostly by decreasing the frame weight. An additional advantage of the relatively tall energy absorbing system was its tendency to satisfy one of the supplementary requirements, namely, prevention of excessive penetration of the landing surface.

With respect to tip-over stability, however, the tall landing system and relatively low outreach were expected to be harmful, and the initial test results indicated how harmful they were. The original model tipped over at less than 3° ground slope when dropped from any significant height. This was considered unsatisfactory, and the remainder of the development program was devoted to improving tip-over stability while the resulting η losses were held as low as possible. Specifically, the weight of the energy absorbing system was held constant since a weight ratio of 0.048 was considered an upper limit, and the η losses were confined to losses in energy absorption.

The original landing system was quite similar to that of figure 1 except that the positions of the present "ski-pole" cutters were occupied by circular aluminum disks which crushed solid plastic foam. Although crushing absorbed the maximum energy from the foam, it had been anticipated that the bounce-back associated with crushing would be harmful to tip-over stability. Hence, when the tip-over results proved unsatisfactory, the next step was to absorb energy by the cutting of solid foam. This change maintained the weight ratio of 0.048 and could readily be made.

In auxiliary drop tests with single cutters, the foam cutting reduced bounce-back by a factor ranging from 4 to 8 depending on the impact velocity

and the nature of the foam and the cutters. The effect of such a bounce-back reduction on tip-over stability is illustrated by the qualitative result curves in sketch (a). The areas between the curves and the axes represent values of vertical impact velocity, V, and ground slope, α, for which the model does not tip over. Curve B is for the cutting of solid foam and is clearly superior to curve A, which is for the crushing of solid foam. The two curves have the same α value for $V = 0$ because the foam height was the same for this comparison. Both curves show α decreasing as V increases because the higher forces associated with the higher velocities give higher bounce-back of the landing system and the landing surface.

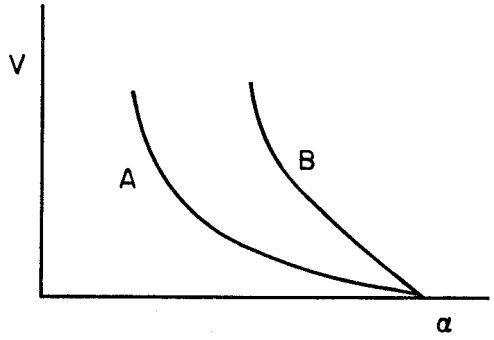

Sketch (a)

The cutting of a given piece of foam must obviously occur at a lower load than the crushing of a similar piece, and this reduces the foam mechanism efficiency, η_M, by a factor of roughly 3 between the initial and final configurations. The primary step taken to hold the loss to this value was to carefully match the foam and its support structure. Many types of foam and many types of cutters, including several sizes of honeycomb, were tried before a combination was found that would always cut and not crush, yet do so at a reasonably high load, (i.e., a reasonably high η_M). In addition, the cutters and their supports were arranged in such a way as to minimize the attachment structure and to utilize in the cutting operation not only the complete cutters but also the attachments, the tension members, and the compression members. (See figs. 1, 2, and 4. The slanted barbs in figs. 1 and 4(b) not only decreased bounce-back but also increased the cutting load.)

In an attempt to improve stability still further, the originally solid foam was hollowed out and lengthened, with the foam volume held constant, to hollow cylinders as shown in figure 4(c). The foam area to be cut was actually tapered so that it approached a maximum at the bottom of the foam.

The foam tapering gave a load-displacement curve for the cutting as shown in sketch (b). The high slope near zero load in sketch (b) resulted from the nearly uniform cutting action of the circular rim of the cutters and provided a large part of the energy area under the load-displacement curve. The longer and lower slope at higher loads resulted from the spokes of the cutters cutting into more and more foam as the displacement increased. This long and low slope permitted "hill accommodation" at relatively low loads. ("Hill accommodation" means that the three foam pads adjust to the ground slope with little deviation of the vehicle axis from the vertical.) The maximum load in sketch (b) was made the buckling load of the frame in order to trigger buckling.

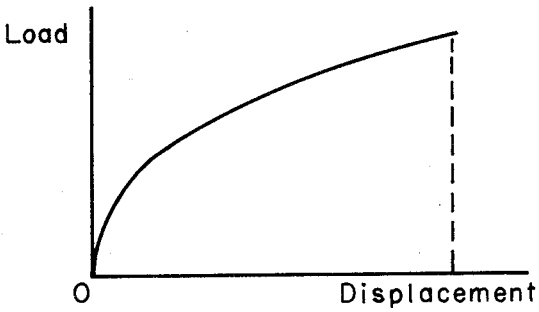

Sketch (b)

The load displacement curve of sketch (b) resulted in the stability curve C shown in sketch (c). The qualitative curve B is reproduced from sketch (a) for comparison purposes. At zero velocity, the stability boundary was lowered in going from curve B to curve C because the center of gravity of the system has been raised by the longer foam pads. The two curves intersected, however, because the hill accommodation mentioned above became the dominant factor at the higher impact velocities; and the resulting boundary C is nearly uniformly restrictive in α over the full range of impact velocities for foam cutting. The stable angles are generally greater for curve C than for curve B. Moreover, this improvement in stability was achieved with only a minor loss in η.

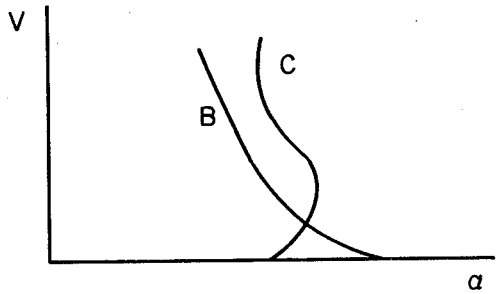

Sketch (c)

Results and Discussion

Results on energy absorption and tip-over stability for the final model configuration (fig. 1) are presented in figure 6 and show envelopes extending from the α axis to the V axis, where α is the landing surface slope in degrees and V the vertical impact velocity in feet per second. Within the envelope, the model does not tip over, and the resultant acceleration does not exceed 50 earth g. This figure scales to 5 earth g for a prototype with 10 to 1 scaling, as shown in equation (A6). This acceleration limit seems to be satisfactory since reference 29 suggests a range from 4 to 8 g.

All the data in figure 6 are expressed in terms of symbols denoting various degrees of tip-over stability or instability. The phrase "very stable" means the model may tip a little but rights itself without hesitation. On the other hand, "barely stable" means the model tips, hesitates, and then rights itself. A designation of "barely unstable" means the model tips, hesitates, and then tips over, while "very unstable" means the model tips over without hesitation.

In figure 6(a), the end point of the solid line on the α axis at $8\text{-}1/2^{\circ}$ is the stability point when only the uphill foam touches the ground prior to release of the model. The end point on the V axis, at 41 ft/sec, is the point at which the system goes above 50 g on a horizontal surface. When this velocity is squared and divided by a denominator consisting of 2 g times the ratio of the system weight to the total landing weight, that is, a denominator of 2 g (0.048), the result is the over-all efficiency of energy absorption, η, specifically, 545 ft-lb/lb. (Note that this value does not include the weight or energy absorption of any mechanism for foaming the plastic or any cover into which it could be foamed for a full-scale vehicle. These effects would probably not be of major importance.)

Whether such an η value is high or low depends on a comparison with competitive systems from references 3 to 33. A system is considered

competitive if it includes a frame to extend the system outboard of the landing vehicle and if it has been found reasonably satisfactory with respect to tip-over stability for a model vehicle somewhat similar to the present model. Unfortunately, numbers from which η values can be found are available only for one such system, specifically, the system described in references 12 and 20. These numbers indicate an over-all efficiency approximately one-half as high as the present value of 545 ft-lb/lb. The η comparison just given suggests that the present system has exceptionally good over-all efficiency. (A comparison on tip-over stability will be given later.)

The end points just described for the solid line in figure 6(a) determine the desired stability envelope, namely, the dashed rectangle. It is presented to illustrate the relatively small extent to which the present boundary deviates from being uniformly restrictive. The lower part of the boundary results from the foam cutting process and has been made nearly vertical by the methods described earlier. Specifically, hill accommodation predominates at a velocity of 4 ft/sec, with bounce-back gradually reducing the stability at higher velocities. The slight recovery in stability above 32 ft/sec, however, is associated with the onset of frame buckling, which releases the impact load with increasing deflection and thus reduces bounce-back.

As a result of this nearly vertical stability boundary, together with the foam cutting, the minimum landing surface slope on the wavy solid line in figure 6(a) is $6\text{-}1/2^\circ$ for all but the highest velocities, rather than the original minimum of less than 3°. As might be expected, the minimum surface slope for impacts with two legs uphill, as defined by the wavy dashed line and flagged symbols in figure 6(a), is considerably higher than $6\text{-}1/2^\circ$.

Figure 6(b) contains energy and tip-over results for vertical impacts on the steel surface described earlier. Since the end point on the velocity axis is the same as for figure 6(a), the over-all efficiency retains the same high value. With respect to tip-over stability, however, the minimum landing surface slope is reduced to $5\text{-}1/4^\circ$ in figure 6(b). This loss of stability can be attributed to increased bounce-back of the steel surface relative to the basalt surface and/or to decreased hill accommodation by the steel surface because it cannot be permanently indented by the foam pads. These detrimental factors apparently predominate over any benefit which might result from the coefficient of static friction, μ, between the model and the steel being lower than that between the model and the basalt (specifically, $\mu = 0.59$ for steel; and $\mu = 0.65$ and 0.72 for basalt, with the model imbedded 1/3 inch and 1/2 inch, respectively).

It should be mentioned that the present results apply to the present ground simulations. Because of the relatively low mass and clean support of the present platform, it seems likely to produce a greater bounce-back stroke than the lunar surface. Hence, the present results are considered conservative.

Results for nonvertical impacts on crushed basalt are presented in figure 6(c). The downhill slope of the landing platform is in the direction of the horizontal component of velocity, and the data are for one leg uphill. Hence these results represent the most critical condition considered herein for tip-over stability on the basalt surface.

The results of figure 6(c) are given for a nominal impact flight-path angle, β, of 85° above the horizontal. Actual angles are given in parentheses near the data points. For a comment on the small deviations from 85° and the fairing of the curve in this figure, see the end of appendix B. Note that the stable region for $\beta = 85^\circ$ is considerably smaller than the stable regions in figures 6(a) and 6(b), which correspond to $\beta = 90^\circ$. Hence it is concluded that the present combination of landing vehicle and energy absorbing system is restricted, by stability considerations, to nearly vertical impacts.

By comparison, the model of references 12 and 20 is not restricted to nearly vertical impacts. It can, in fact, accept downhill horizontal velocities on a 5° slope in the order of 8 to 10 ft/sec over a vertical velocity range from 0 to 14 ft/sec. Thus the landing system of references 12 and 20, while having a lower over-all efficiency, η, than the present system by a factor of 2, is considerably better with respect to tip-over stability. The system of references 12 and 20 is intended to meet the full range of requirements in references 12 and 49 (which include a vertical velocity requirement but no specification on η). On the other hand, the present system is intended to exceed the vertical velocity requirement but to meet only one of the stability requirements, namely, the specification of a 5° ground slope for otherwise vertically symmetrical impacts; and this has been accomplished, as seen in figures 6(a) and 6(b).

Although the present criterion for η is a perfectly symmetrical landing, it is of some interest to consider a more critical condition. This is the case where the impact is nonvertical with the horizontal velocity component directed uphill, where tip-over is prevented by the steepness of the ground slope, and where the model is oriented with one leg uphill. This orientation provides the least protection for the uphill leg and hence the maximum likelihood of the acceleration exceeding 50 g. The maximum resultant velocity achievable with the existing rail length was 35.6 ft/sec at a β of 80° above the horizontal, and the ground slope for this case was 21°. The model acceleration still did not exceed 50 g. A velocity of 35.6 ft/sec means that η for the nonvertical impacts is at least 411 ft-lb/lb, as opposed to 545 ft-lb/lb for the symmetrical impacts.

Thus the present configuration is efficient even for a slightly nonvertical impact into a 21° hill. It is significant that this is so despite the use of a relatively heavy energy absorbing mechanism having a low mechanism efficiency, η_M. Specifically, the foam comprises almost half the weight of the present system; and the foam cutting mechanism has an η_M value of 777 ft-lb/lb, which is much lower than most of the mechanism efficiencies listed in reference 29. Possible effects of the space environment and rocket exhaust on the η_M values for foam crushing and foam cutting are considered in appendix C.

CONCLUDING REMARKS

An energy absorbing system for space-vehicle landings has been described and experimentally evaluated. Plastic foam was investigated as the main energy

absorber because it could be expanded to a large volume after exit from the earth's atmosphere and thus help prevent excessive penetration of the landing surface without causing a major packaging problem. The system has an aluminum frame to support the foam and three legs to improve blast-off stability for the return flight.

An attempt has been made to utilize the selected materials so as to improve tip-over stability and over-all efficiency of energy absorption. Priority has been given to efficiency, and it has been improved in three ways. First, the frame has been designed with relatively low outreach beyond the body perimeter. Secondly, the frame has been designed to absorb energy by buckling, and third, the foam has been carefully matched to its support structure.

The efficiency was compromised partially to improve tip-over stability. The compromise consisted of absorbing energy from the foam by cutting it instead of crushing it. This has improved stability by decreasing bounce-back but resulted in a significant efficiency loss. Stability was also improved by adjusting the system so that the stability boundary is almost uniformly restrictive on ground slope over the full range of impact velocities. This adjustment resulted in only a minor loss of over-all efficiency.

Despite the very low mechanism efficiency of cutting the foam (777 ft-lb/lb), the steps just outlined resulted in an over-all efficiency which is considered exceptionally good, specifically, 545 ft-lb/lb. The tip-over stability results have been less satisfactory, with the vehicle restricted to a 5° ground slope and nearly vertical impacts.

Ames Research Center
National Aeronautics and Space Administration
Moffett Field, Calif., July 8, 1965

APPENDIX A

SCALING

The scaling used herein is derived from two conditions: (1) the model is scaled geometrically relative to the prototype; and (2) the model is made from the same material as the prototype, which requires identical stresses and identical material densities. From condition (1), with N taken as a fixed number,

$$\frac{L_p}{L_m} = N, \qquad \frac{A_p}{A_m} = N^2, \qquad \frac{v_p}{v_m} = N^3 \tag{A1}$$

where L, A, and v are length, area, and volume, respectively, and where the subscripts p and m stand for prototype and model. From the identical stress aspect of condition (2), together with equation (A1),

$$\frac{F_p}{A_p} = \frac{F_m}{A_m}, \qquad \frac{F_p}{F_m} = N^2 \tag{A2}$$

where F is force. From the identical material density aspect of condition (2), together with equation (A1),

$$\frac{M_p}{v_p} = \frac{M_m}{v_m}, \qquad \frac{M_p}{M_m} = N^3 \tag{A3}$$

where M is mass.

An immediate question is whether the weight force, W, is consistent with equation (A2). For this force, with equation (A3),

$$\frac{W_p}{W_m} = \left(\frac{M_p}{M_m}\right)\left(\frac{g_p}{g_m}\right) = N^3 \frac{g_p}{g_m} \tag{A4}$$

where g is acceleration due to gravity. Hence, for consistency with equation (A2), it must follow that

$$\frac{g_p}{g_m} = \frac{1}{N} \tag{A5}$$

If the prototype is to land on the moon and the model is to be tested on earth, equation (A5) requires that $N = 6$ for exact scaling of the weight force.

Other quantities follow directly from equations (A1) to (A3) in conjunction with specific laws of nature. For example, the same development

yielding equation (A5) gives

$$\frac{a_p}{a_m} = \frac{1}{N} \tag{A6}$$

where a is acceleration. Equations (A5) and (A6) serve different functions, with equation (A6) scaling accelerations according to any number N and equation (A5) specifying N according to the physical accelerations due to gravity.

For scaling the dimensions of velocity, V, the formula for constant acceleration, $V^2 = 2aS$, can be used, where S is the distance over which constant acceleration takes place. With equations (A1) and (A6), it is seen that (with general length, L, specialized as S)

$$\frac{V_p^2}{V_m^2} = \frac{a_p S_p}{a_m S_m} = \left(\frac{1}{N}\right)\left(N\right) = 1 \tag{A7}$$

For time scaling, another formula for constant acceleration, $V = at$, can be used, where t is time. Equations (A6) and (A7) then give

$$\frac{t_p}{t_m} = \left(\frac{V_p}{a_p}\right)\left(\frac{a_m}{V_m}\right) = N \tag{A8}$$

Equations (A1) through (A8) have been checked by other physical laws and relations, including work-energy, impulse-momentum, torque-inertia, and stress-bending moment.

A question arises as to what happens when the restriction in equation (A5) is lifted. First, if N is within a factor of 2, say, of that determined by equation (A5), there is no problem in scaling forces as long as the maximum deceleration force is greater than the weight force by a factor of, say, 20 or more. Secondly, with respect to stability, the model results would be exact for a prototype with $N = 10$ if the lunar gravitational acceleration were 1/10 that of the earth rather than 1/6. Thus the prototype on the moon is subjected to a stronger gravity force than is the model on earth. The prototype is, therefore, less likely to tip over than the model, both with respect to bounce height and gravity restoring moment. In this sense, the model results are considered conservative as to stability for a prototype with $N = 10$.

Hence, it seems justified to consider $N = 10$ as well as $N = 6$; and $N = 10$ comes closer to the actual Lunar Excursion Module, or LEM, for the model described in the body of the report. When this model is scaled according to equations (A4), (A6), and (A1), the result is

N = 6

$$\left.\begin{aligned} W_p &= 35.08\ (6)^3 = 7580 \text{ lb on earth} \\ n_p &= \frac{50}{6} = 8.3 \text{ earth g} \\ d_p &= \frac{14.4}{12}\ (6) = 7.2 \text{ ft} \end{aligned}\right\} \qquad (A9)$$

N = 10

$$\left.\begin{aligned} W_p &= 35.08\ (10)^3 = 35{,}080 \text{ lb on earth} \\ n_p &= \frac{50}{10} = 5 \text{ earth g} \\ d_p &= \frac{14.4}{12}\ (10) = 12 \text{ ft} \end{aligned}\right\} \qquad (A10)$$

where d_p is the diameter of the prototype body and n_p is the maximum earth load factor.

The scaling of the plastic foam is initially troublesome because the foam cell diameter and the model cutter thickness are the same order of magnitude, and because the foam cells may not be appreciably larger for the prototype. It may be desirable, then, to scale the number of cutters rather than the thickness of the cutters. Then the cutting force should scale properly, according to the total cutting area and this area could readily be scaled according to N^2, as required.

APPENDIX B

APPARATUS AND ERROR ESTIMATION

One channel of the system for measuring acceleration is shown in sketch (d). The dc amplifier is used primarily to boost the signal, its gain being set permanently at 100. The other two amplifiers are used mainly for impedance

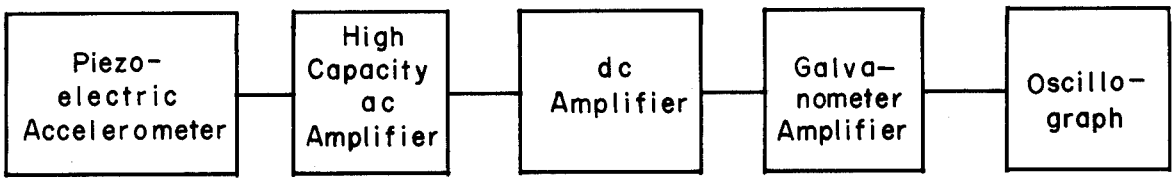

Sketch (d)

matching. The gain of the ac amplifier is set at unity to minimize the network time constant and resulting overshoot, and the galvanometer amplifier provides a smoothly adjustable gain for convenience in displaying a trace on the oscillograph paper.

Before each test an electrical calibration is performed by replacing each accelerometer by a prescribed sinusoidal voltage from a signal generator. The voltage level corresponds to a specified acceleration. The gain of the galvanometer amplifier is then adjusted to give the largest feasible amplitude on the oscillograph paper. This recorded signal constitutes the calibration for the specified acceleration and effectively removes the effect of any gain drift in the measuring system. It would not remove the effect of deviations in overshoot, but the overshoot has been reduced to considerably less than 1 percent.

The prescribed voltage level for the electrical calibration was obtained by using the system to measure a known acceleration, specifically, 60 g. The accelerometers were placed on a shake table capable of delivering 60 g acceleration at a frequency as low as 130 cps. The frequency selected for the known acceleration was 200 cps, as measured by a counter. The shaker displacement amplitude was set to deliver 60 g at 200 cps, the amplitude being measured by an optical displacement follower as checked against a bench micrometer. The gain of the galvanometer amplifier was adjusted to display traces of convenient size on the oscillograph paper, and then the gain was locked. Each accelerometer was replaced in turn by a signal generator, and the voltage level of the generator was adjusted until the oscillograph trace matched the corresponding trace produced by the shaker. This voltage level constituted the electrical calibration.

There is, of course, a certain amount of error involved in the determination and performance of the electrical calibration; and this error has been evaluated on the basis of the various readings and meters involved. Another error, due to variations from the frequency of 200 cps, has been estimated by means of a frequency response with the accelerometers mounted on the shake table. A third error arises from a slight lack of linearity and has been

evaluated by comparing a 60 g frequency response with a 30 g response. A fourth error results from the estimation of a mean line through 1000 cps oscillations of relatively low amplitude, which are superimposed on the acceleration traces and are regarded as unimportant because of their high frequency.

When the four error estimates just referred to are added, the total is 8 percent. This defines the maximum possible acceleration error. When the square root of the sum of the squares of the individual errors is taken, with the electrical calibration broken into its components, the resulting standard deviation is 3 percent.

Another potential source of error in the over-all test program involves variation in the energy absorbing system from model to model. With respect to the plastic foam, however, there could not have been much variation since the tip-over results below the frame buckling load turned out to be highly repeatable in general. (It should be noted that the maintenance of good repeatability and minimum bounce-back required the axis of every pad cut from every foam log to be oriented in a specific direction relative to the log geometry.)

Above the frame buckling load, tip-over repeatability could not be checked because of a shortage of models. For six perfectly symmetrical impacts, however, the maximum deviation from the average buckling load was 7 percent. In addition, frame buckling affects only the extreme top of the measured stability envelopes of figure 6. On the basis of the foregoing information, it is considered that variations in the foam and the frame could result in only minor errors in the envelopes.

The remaining sources of error apply only to the nonvertical impacts, and this leads to a description of the rails shown in figure 3. The working part of each rail consists of a channel completely lined with a damping material. The interior height of the channel, when lined, is 1-1/8 inch, or 1/8 inch greater than the diameter of the model runners. In the lateral direction, the model runners are 1/8 inch from the interior channel lining when the model is centered between the rails, and the rails are 36-3/4 inches apart from interior lining to interior lining. The lining material is slow rebound silicone rubber, 1/8 inch thick. It is painted with a dispersion of fluorocarbon powder to decrease friction, and its purpose, of course, is to minimize oscillations of the model.

Possibly as a result of this precaution, together with the location of the model runners, release mechanism, and center of gravity in a single plane, the model slides down the rails without observable oscillation. In addition, the tip-over results for nonvertical impacts are generally repeatable. Hence, the error due to oscillations is considered small.

Two possible sources of unwanted pitching velocity remain, however, as the model comes off the rails. These are a gravity moment and the hitting of the rails by the runners due to gravity free fall. To minimize the gravity moment, the model runners have been recessed 3/16 inch over the aft 5-1/2 inches of their length, as shown in the sketch in figure 4(a). Hence there can be no gravity moment after the model center of gravity is 1-1/2 inches beyond the end of the rails, and calculations indicate a resulting maximum pitching

velocity of 0.014 radian per second for the test conditions reported in figure 6(c). Such a pitching velocity should introduce only a negligible error in a tip-over stability boundary.

After the center of gravity is more than 1-1/2 inches beyond the rails, the model is in a free-fall state, and the 3/16-inch recess, selected for convenience in model construction, is not deep enough to preclude the possibility of the aft end of the runners ticking the end of the rails. Calculations, however, indicate that such ticking of the rails takes place only for one of the data points in figure 6(c). Since this data point represents a stable condition, there is little error in the stability boundary as a result of rail ticking.

The model velocities for the gravity moment and rail ticking calculations, as well as the initial free-fall velocity for determining the impact speed and flight path, are taken from high-speed motion pictures of the model sliding down the rails. Distance versus time is plotted on the basis of the stripes on the rails, the pointer on the model, and timing marks on the film. The slope of the plot gives the resultant velocity in the direction of the rails. The slope is determined both by graphical estimation and by taking the derivative of a least-squares parabolic fit. Graphical estimation is used when the graph is linear over a wide range surrounding the point where the slope is desired. Otherwise, an average is taken between the slopes determined by estimation and least squares.

For the resultant velocity just as the model goes into free fall, the average slope differs from those of estimation and least squares by a maximum of 10 percent. Among the four remaining data points of figure 6(c) for which an average was taken, however, the maximum error is 2 percent. Since the velocity at the start of free fall is the initial velocity for calculating the impact speed, that speed is considered to have a maximum error of less than those indicated above. (A much lower error is indicated for the purely free-fall vertical impacts by comparison of calculations and high-speed movies of the model and a striped backboard. This comparison shows essentially no effect of air drag on the free-fall velocities.)

With respect to the flight-path angle for nonvertical impacts, the initial free-fall velocity errors just described should cause no significant errors in the predicted impact angles. Because the model was in free fall for 6 inches, however, those predicted angles do differ somewhat from the nominal flight-path angle of 85°, which is the angle at which the rails are set. This variation causes the plotted points of figure 6(c) to be somewhat unconservative for an 85° slope. Hence, the stability boundary is faired more conservatively than the data points, particularly at the lowest impact speeds. This procedure obviously causes some error for the boundary.

APPENDIX C

AUXILIARY TESTS ON VACUUM AND TEMPERATURE

The experiments described in the body of the report were performed at room temperature and pressure and hence did not account for the effects of foam exposure to the space environment. As a partial check on the effect of this environment, plastic foam has been tested in a vacuum bell jar and at low temperature. Load-deflection tests were performed on the crushing and the cutting of foam, where the load was measured by a load cell and the deflection by a differential transformer-type transducer.

The model for the crushing test was a 5-1/2-inch-diameter sphere of polystyrene foam, with a density of 1.8 lb/cu ft. Its load-deflection curve was first found at room temperature and pressure. Then the bell jar was pumped down to 10^{-5} mm of mercury (torr) at room temperature and held there for 5 minutes. This part of the test showed that the foam will not explode in a vacuum. Then the foam was crushed at the same rate[1] as for room temperature and pressure. The result was a load ranging from one-half to one-third as great as the load for room conditions, as seen in figure 7. Not all the air had been removed from the foam by the evacuation of the bell jar since the pressure went up during the crushing, but enough had apparently been removed to lower the load as indicated.

The crushing test was then repeated at room pressure, but this time the specimen was a 5-1/2-inch-diameter polystyrene sphere which had been held in liquid nitrogen at -170° F for 5 minutes. The result, as seen in figure 7, was a load-deflection curve almost identical to that for the vacuum case. Calculations indicate the low temperature reduced the load relative to room conditions by lowering the air pressure in the foam cells and also by lowering the strength of the plastic material.

A glance at the areas under the curves in figure 7 indicates that the energy absorbed in vacuum and at low temperature is approximately half as great as at room temperature and pressure. This fact would have to be accounted for in any design based on the crushing of foam.

Similar tests were performed for foam cutting. The foam model was that described in figure 4 except that 4 inches were cut off the open (upper) end and 2 inches off the outside diameter to make the foam fit in the test rig.

---

[1]The importance of crushing rate for polystyrene spheres with a density of 1.8 lb/cu ft was established by an earlier test at room temperature and pressure. In this test the static load at a given deflection of a 5-1/2-inch-diameter sphere was found to be lower by a factor of 2 than the corresponding dynamic load when the crushing rate was varying from 55 ft/sec to roughly half that value. In contrast, the rate effect was found to be relatively small in reference 21 for rectangular volumes of polystyrene.

The cutter was identical to those of figure 1 and figure 4, with a simulated support frame. The rim of the cutter missed the foam because of the reduction in the foam outside diameter.

For the vacuum case, the model was held at 1.5×10^{-5} mm of mercury for 24 hours before the load-deflection test was performed. Again the bell jar pressure went up during the loading, indicating that some air remained in the foam. For the low temperature case, the model was held in liquid nitrogen at -170° F for approximately 3 minutes.

Load-deflection results for foam cutting are represented by square symbols in figures 8 and 9 for vacuum and low temperature, respectively. The circular symbols in these figures are for room temperature and pressure. The small difference between the two curves for room conditions may result from the fact that the foam reported in figure 8 comes from a different log than that in figure 9.

From 0 to almost 2 inches deflection in figures 8 and 9, the load is due almost entirely to foam cutting because, for these deflections, the cutters are widely spaced in the foam, and the crushing by the frame is negligible. Within this nearly pure cutting region, the loads for the vacuum case in figure 8 and the low temperature case in figure 9 are almost as large as the corresponding loads for room conditions. Hence the energy loss due to environment is negligible for cutting as compared to that for crushing.

For deflection greater than 2 inches, the load is partly due to cutting and partly due to crushing by the simulated frame members. Differences between figures 8 and 9 may be due to different effects of vacuum and temperature, or they may be due to a coincidental difference in the breaking out of the side wall of the hollow foam cylinder.

The foregoing results have not, of course, included the effect of high temperature resulting from a space environment or the rocket exhaust. In this connection, the plastic material would probably have to be foamed into a cover to achieve the required temperature and pressure for foaming a dependably brittle product; and such a cover would provide some protection against high temperature, or low temperature. (It should be noted that the details of the foaming process are beyond the scope of the present report.) With respect to the rocket exhaust, the nozzle could be made long enough so that the exhaust misses the plastic foam.

REFERENCES

1. NASA Research Advisory Committee on Structural Design: Important Research Problems in Advanced Flight Structures Design - 1960. NASA TN D-518, 1960.

2. NASA Research Advisory Committee on Missile and Space Vehicle Structures: Important Structural Research Problems for the Support of Future Space Missions. NASA TN D-2059, 1963.

3. Flora, C. L.: Impact Deceleration Systems Applicable to Lunar Landing Vehicles. Rep. 2324, Radioplane, Div. of Northrop Corp., Nov. 1960.

4. Goldstone, N. J.: Landing Shock-Absorption. Proc. Inst. Environ. Sci. Natl. Meeting, Washington, D. C., April 5-7, 1961, pp. 215-224. I.E.S., Mount Prospect, Ill.

5. Feigen, M., Fitzgibbon, D., and Burchman, E.: Characteristics of Energy Absorbing Materials for a Lunar Soft Landing Vehicle. 9753-0001-MU-000, EM 11-17, Space Technol. Lab., Inc., Aug. 1961.

6. Lindberg, H. E.: Stability of Cushioned Lunar Landing. Rep. 6-90-61-87, Lockheed Missiles and Space Div., Sept. 1961.

7. Gallagher, A. E., and Ingelse, A. O.: Drop Tests Prove Out Inflatable Lunar Decelerators. Part 1, Space/Aeronautics, Nov. 1961, pp. 69-71.

8. Duke, William M.: Lunar Landing Problems. Vol. X, Manned Lunar Flight. In: Advances in the Astronautical Sciences, Western Periodicals Co., North Hollywood, Calif., 1963, pp. 39-51. Also Am. Astronaut. Soc., Symp. on Manned Lunar Flight, Denver, Colorado, Dec. 1961.

9. Fisher, Lloyd J., Jr.: Landing-Impact-Dissipation Systems. NASA TN D-975, 1961.

10. Forlifer, W. R.: Lunar Landing Module Study, Landing Dynamics. ER-12298, Martin Co., Baltimore, Maryland, Mar. 1962.

11. Stubbs, Sandy M.; and McGehee, John R.: Investigation of the Landing Characteristics of a Reentry Vehicle Having a Canted Multiple-Air-Bag Load-Alleviation System. NASA TN D-1934, 1963.

12. Judge, John F.: Bendix Seeks LEM Landing Contract. Missiles and Rockets, vol. 12, no. 10, Mar. 11, 1963, pp. 26-32.

13. Lavender, Robert E.: Lunar Logistic System. Vol. XI, Lunar Touchdown. MTP-M-63-1, Marshall Space Flight Center, Mar. 1963.

14. Cappelli, A. P.: Dynamic Analysis for Lunar Alightment. AIAA J., vol. 1, no. 5, May 1963, pp. 1119-1125.

15. Burns, Andrew B.; and Plascyk, James A.: Lunar Alightment Systems Investigation. ASD-TDR-63-454, Flight Dynamics Lab., Aero. Systems Div., Air Force Systems Command, Wright-Patterson Air Force Base, Ohio, June 1963.

16. Lavender, Robert E.: Touchdown Dynamics Analysis of Spacecraft for Soft Lunar Landing. NASA TN D-2001, 1964.

17. Anon.: LEM Familarization Manual. LMA 790-1, Grumman Aircraft Engr. Corp., Mar. 15, 1965.

18. Walton, W. C., Jr.; Herr, R. W.; and Leonard, H. W.: Studies of Touchdown Stability for Lunar Landing Vehicles. J. Spacecraft Rockets, vol. 1, no. 5, Sept.-Oct. 1964, pp. 552-556.

19. Blanchard, Ulysse J.: Characteristics of a Lunar Landing Configuration Having Various Multiple-Leg Landing-Gear Arrangements. NASA TN D-2027, 1964.

20. Black, Raymond J.: Quadrupedal Landing Gear Systems for Spacecraft. J. Spacecraft Rockets, vol. 1, no. 2, Mar.-Apr. 1964, pp. 196-203.

21. Turnbow, James W.: Cushioning for Air Drop. Part VII, Characteristics of Foamed Plastics Under Dynamic Loading. Univ. of Texas, Mar. 28, 1957.

22. Matlock, Hudson; Ripperger, E. A.; Turnbow, James W.; and Thompson, J. Neils: Energy-Absorbing Materials and Systems. Shock and Vibration Bull., Part II, Dec. 1957, pp. 305-323.

23. Anon.: Development of Foamed-in-Place Plastic Energy Absorbing Materials. Final Rep., Atlantic Res. Corp., Dec. 31, 1956 to Mar. 31, 1958.

24. Supnik, Ross H.; and Silberberg, Melvin: Properties of Foams and Laminates Under Shock Loading. Reprinted from the Soc. Plastics Engrs. J., vol. 15, no. 1, Jan. 1959, pp. 43-47.

25. O'Bryan, Thomas C.; and Hatch, Howard G., Jr.: Limited Investigation of Crushable Structures for Acceleration Protection of Occupants of Vehicles at Low Impact Speeds. NASA TN D-158, 1959.

26. Esgar, Jack B.; and Morgan, William C.: Analytical Study of Soft Landings on Gas-Filled Bags. NASA TR R-75, 1960.

27. Anon.: Energy Absorption Properties of Aluminum Honeycomb. TSB-110, Hexcel Products, Inc., Jan. 10, 1960.

28. Kroell, C. K.: A Simple, Efficient, One-Shot Energy Absorber. Gen. Motors Res. Lab. Reprinted from Bull. no. 30, Shock, Vibration and Associated Environments Part III, Feb. 1962.

29. Esgar, Jack B.: Survey of Energy-Absorption Devices for Soft Landing of Space Vehicles. NASA TN D-1308, 1962.

30. Howe, John T.: Theory of High-Speed-Impact Attenuation by Gas Bags. NASA TN D-1298, 1962.

31. McFarland, R. K., Jr.: Hexagonal Cell Structures Under Post-Buckling Axial Load. AIAA J., vol. 1, no. 6, June 1963, pp. 1380-1385.

32. Platus, David L.; Cunningham, Patrick J.; Marovich, Frank A.; and Freeman, Holland H.: Concepts of Multiple-Impact Study of Energy Absorption, Third Quart. Progress Rep. 34, Aerospace Res. Assoc., Oct. 1963 to Jan. 1964.

33. Warner, R. W.; and Marble, D. R.: Possible Materials Needs for Energy Absorption in Space-Vehicle Landings. Special Tech. Pub. 379, Symposium on Newer Structural Materials for Aerospace Vehicles, ASTM, 1965, pp. 55-70.

34. Anon.: Proc. of Lunar and Planetary Exploration Colloquium, vol. 1, no. 1, May 13, 1958.

35. Hibbs, Albert R.: A New Look at the Moon. Engr. and Sci. Mag., June 1960.

36. Warner, Brian: The Nature of the Surfaces of the Lunar Maria. Pub. of the Astron. Soc. of the Pacific, vol. 73, no. 434, Oct. 1961, pp. 349-351.

37. Stitt, Leonard E.: Interaction of Highly Underexpanded Jets With Simulated Lunar Surfaces. NASA TN D-1095, 1961.

38. Barabashov, N. P.: Structure of the Moon's Surface and Investigation of the First Photographs of Its Far Side. NASA TT F-8117, 1962.

39. Spady, Amos A., Jr.: An Exploratory Investigation of Jet-Blast Effects on a Dust-Covered Surface at Low Ambient Pressure. NASA TN D-1017, 1962.

40. Gold, T.: Processes on the Lunar Surface. The Moon, Z. Kopal and Z. Mikhailov, eds., Academic Press (New York), 1962, pp. 433-439.

41. Bernett, E. C.; Scott, R. F.; Jaffe, L. D.; Frink, E. P.; and Martens, H. E.: The Bearing Capacity of Simulated Lunar Surfaces in Vacuum. Tech. Rep. 32-326, Jet Propulsion Lab., Aug. 1963.

42. Firsoff, V. A.: Selenological Implications of the South-Australian Ring Structures. Nature, vol. 198, no. 4875, Apr. 6, 1963, pp. 78-79.

43. Hapke, Bruce W.: A Theoretical Photometric Function for the Lunar Surface. J. Geophys. Res., vol. 68, no. 15, Aug. 1, 1963, pp. 4571-4586.

44. Hapke, Bruce; and Van Horn, Hugh: Photometric Studies of Complex Surfaces, With Applications to the Moon. J. Geophys. Res., vol. 68, no. 15, Aug. 1, 1963, pp. 4545-4570.

45. Bensko, J.; Cortez, J. L.; Fields, S. A.; and Weathers, H. M.: Lunar Logistic System. Vol. VIII, Lunar Surface Conditions by Research Projects Division. MTP-M-63-1, Marshall Space Flight Center, Mar. 15, 1963.

46. Cramblit, D. C.: A Consideration of Lunar Surface Ballistics and the Hazards Associated With Spacecraft Landing or Launch Operations. NASA TN D-1526, 1963.

47. Orlova, N. S.; and Gromov, S. V.: Dust Nature of the Lunar Surface and Determining Figure of the Earth Through Gravity Anomalies (trans. into English of 2 articles from Tr. Astron. Observ. (Leninger.), no. 307, 1962, pp. 179-186 and 234-242). Joint Publications Research Service, vol. 20, no. 167, Washington, D. C., July 15, 1963.

48. Hapke, Bruce: Packing Properties of Fine Powders and the Depth of the Lunar Dust Layer. J. Geophys. Res., vol. 69, no. 6, Mar. 15, 1964, pp. 1147-1151.

49. Kovit, Bernard: LEM: Our First True Spacecraft. Space/Aeronautics Mag., Mar. 1963, pp. 76-83.

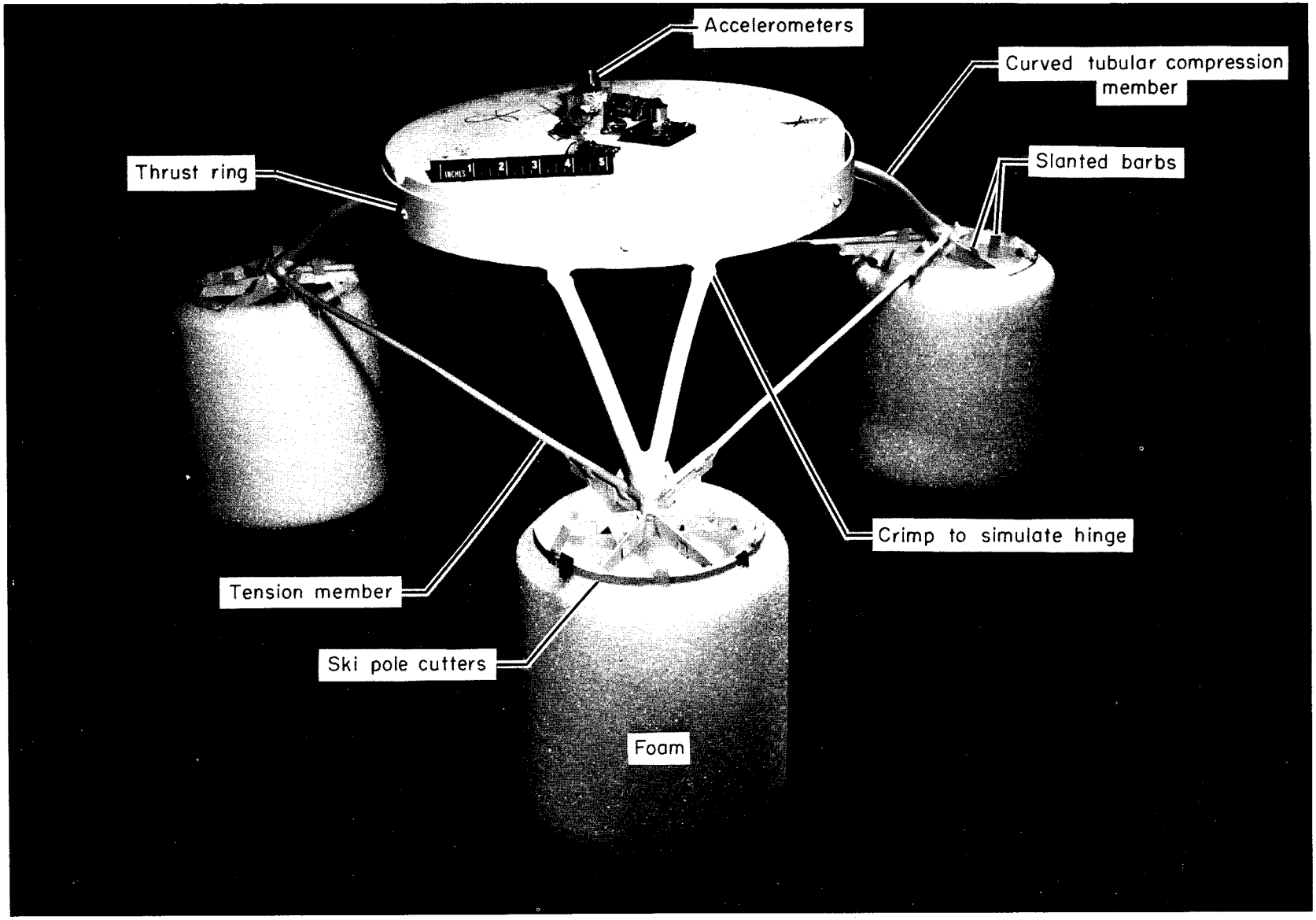

A-32456

Figure 1.- Energy absorbing system.

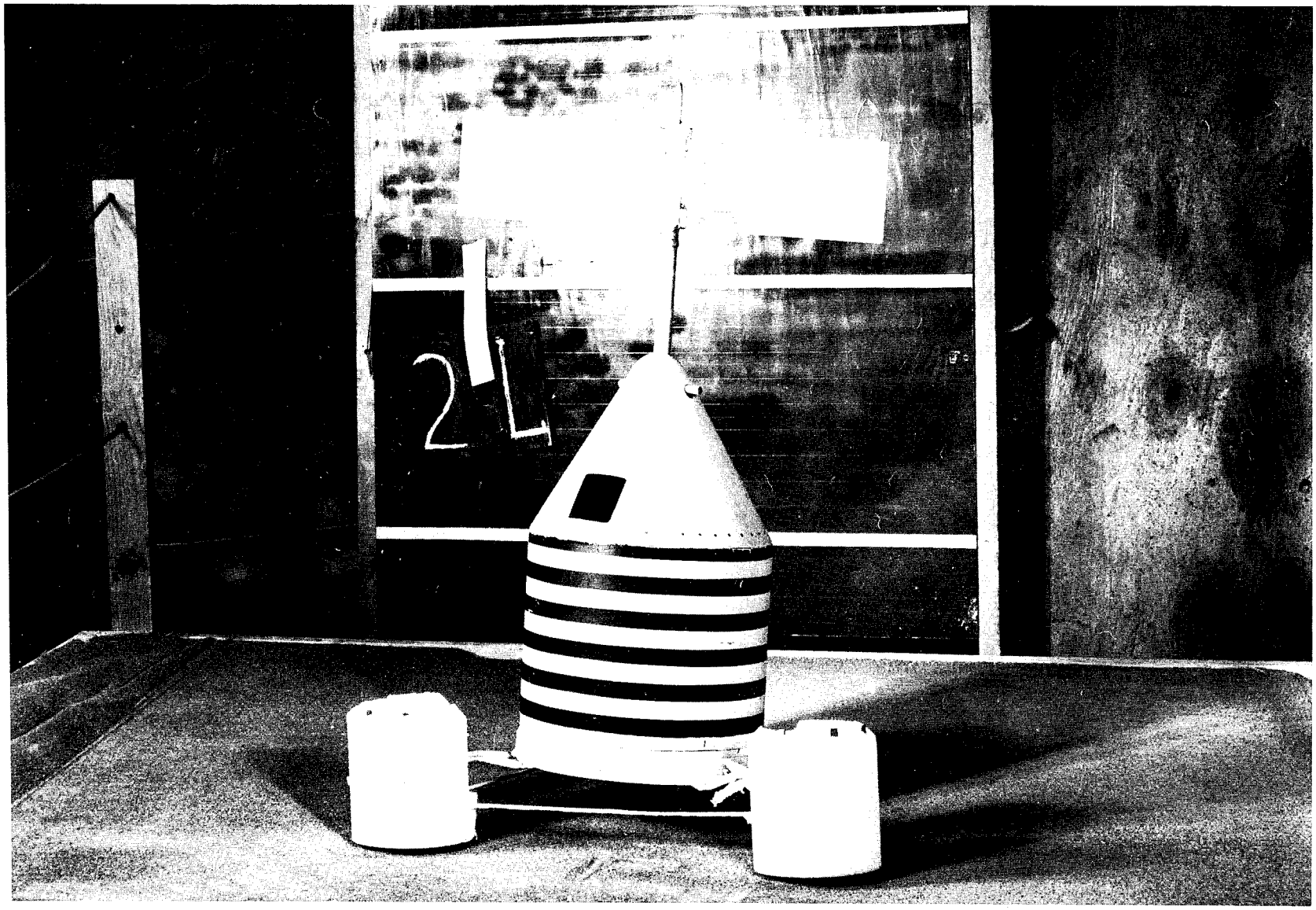

Figure 2.- Test facility for vertical impacts and model after impact.

A-31622

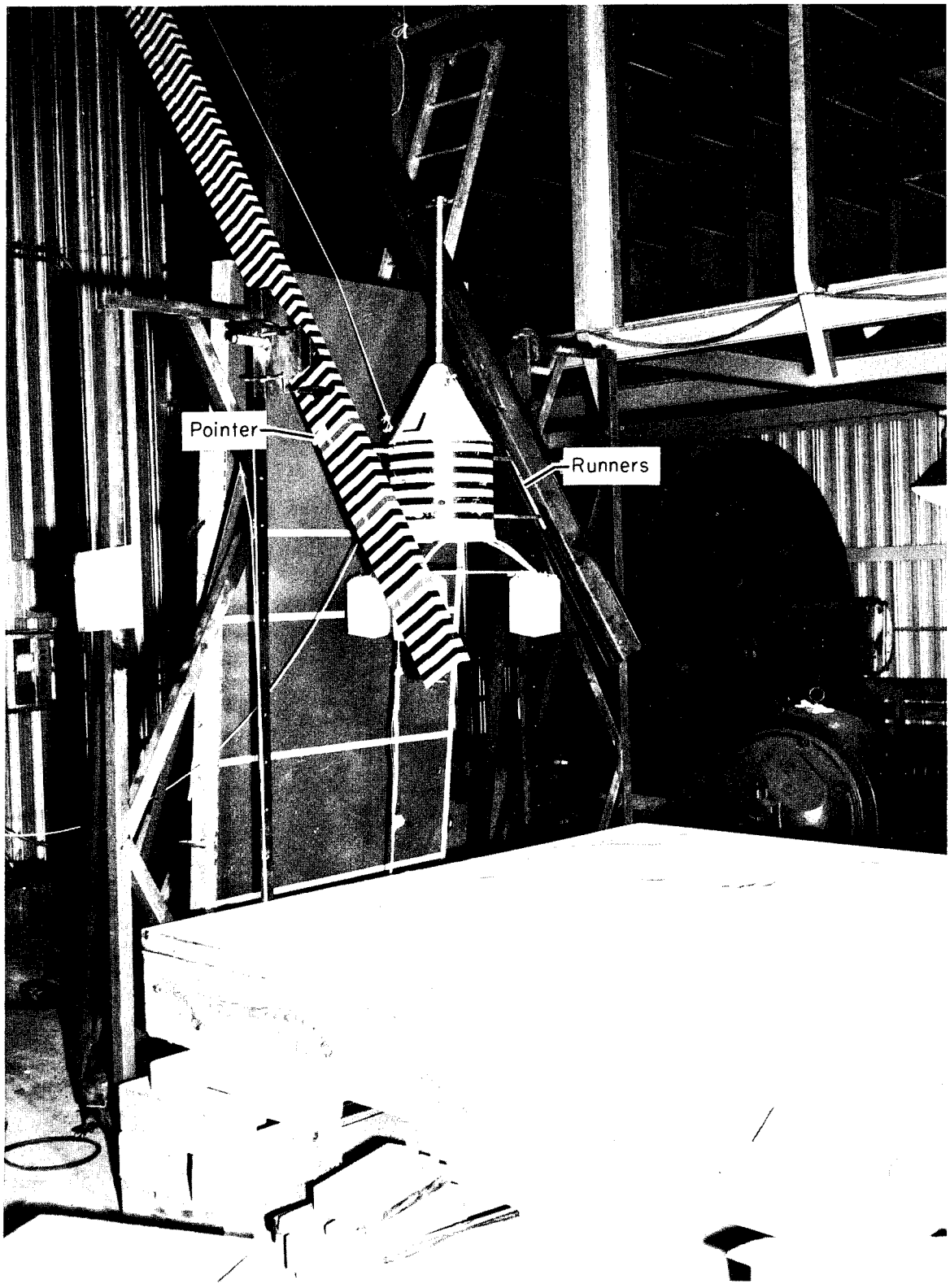

Figure 3.- Test facility for nonvertical impacts. A-33064

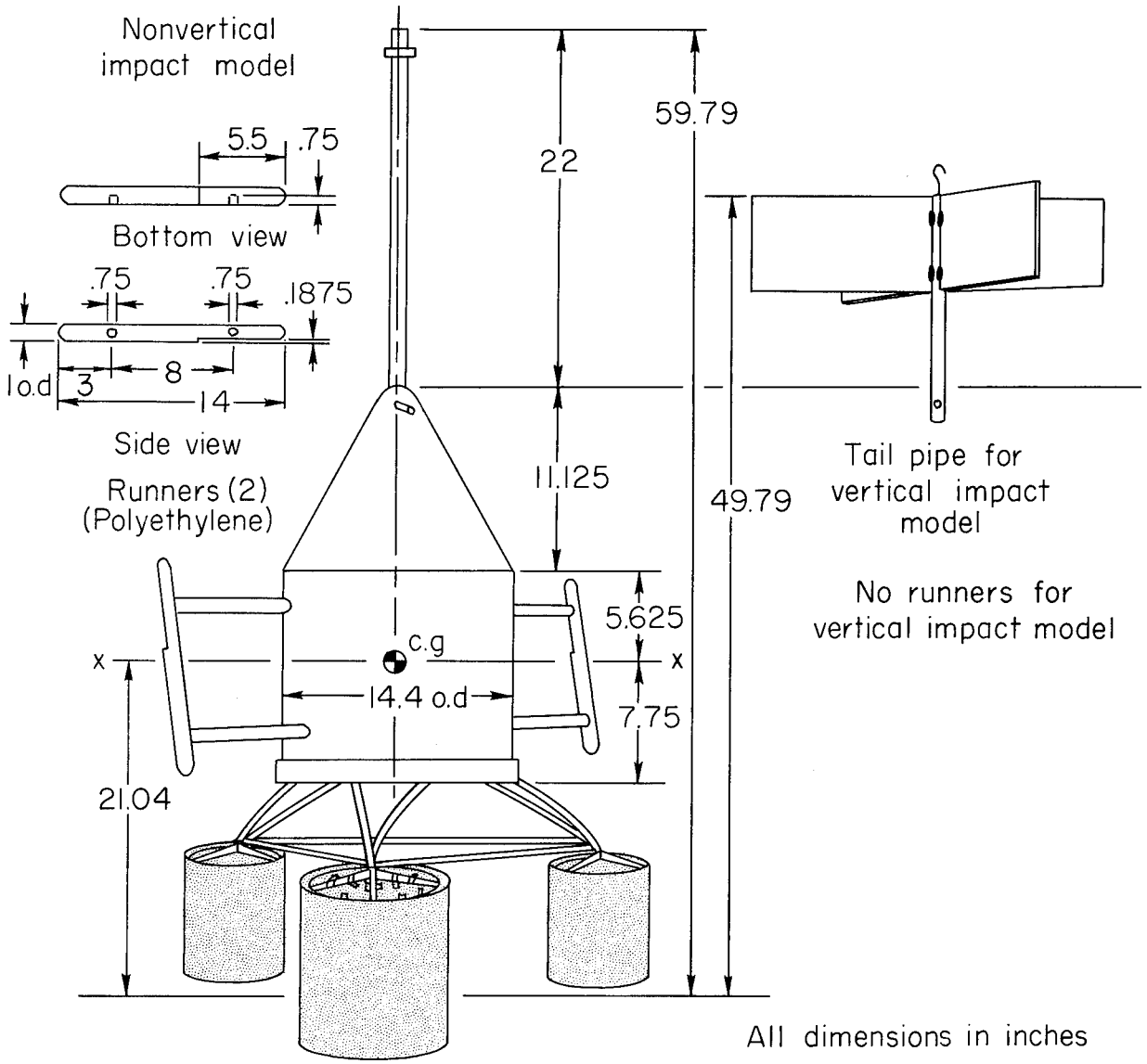

$I_{xx} = 8.22$ in. lb sec^2 for both models

W = 35.07 lb-gross weight for both models

Density = 20.21 lb/ft^3 (model body, fins and thrust ring)

$$\text{Weight ratio} = 0.048 \left(\frac{\text{weight of landing gear}}{\text{gross weight of model}} = \frac{1.68 \text{ lb}}{35.07 \text{ lb}} \right)$$

$$\frac{\text{gross weight, lb}}{\text{max. total foam bearing area, in.}^2} = 0.3 \text{ lb/in.}^2$$

(a) General.

Figure 4.- Model parameters.

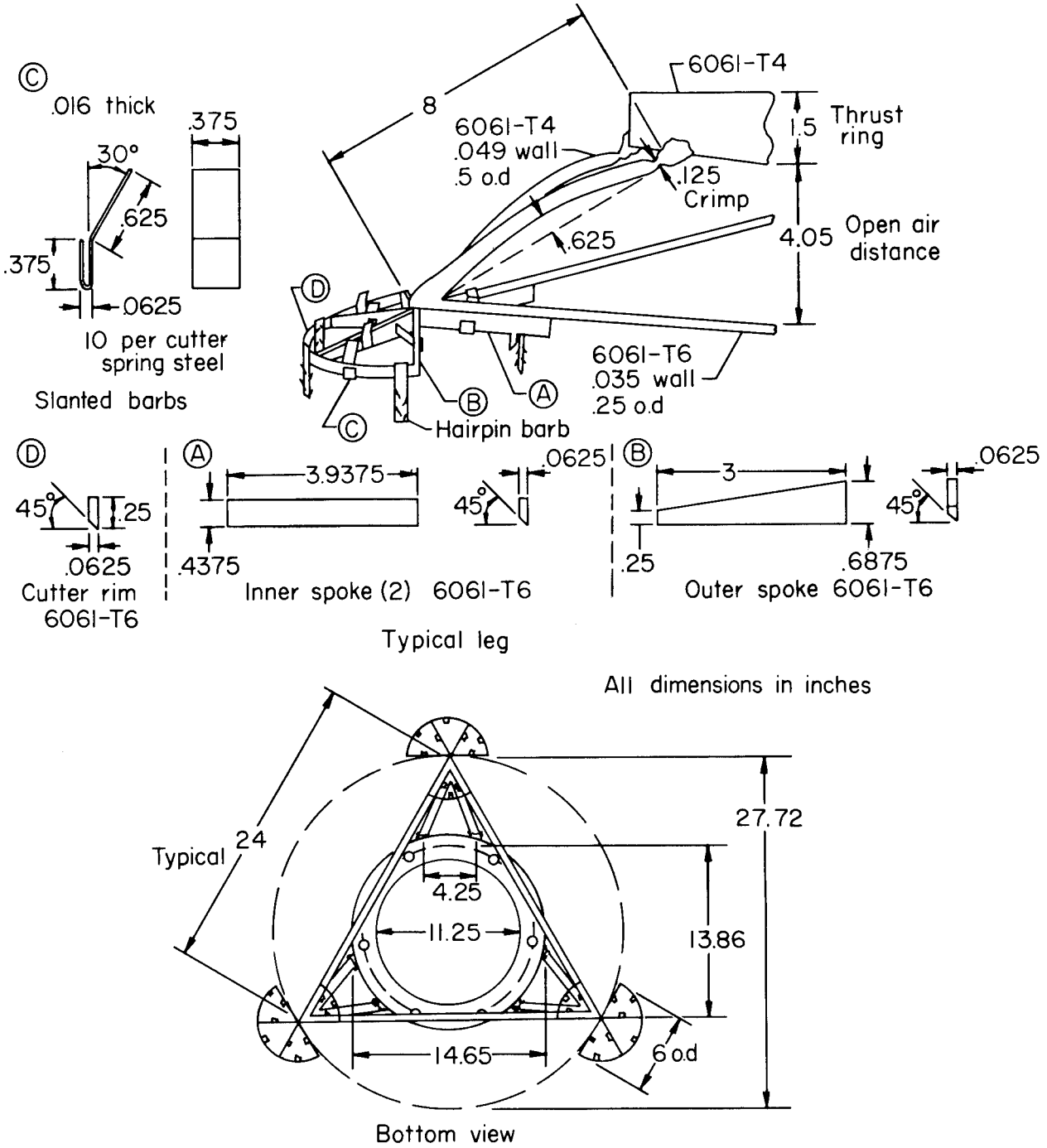

Weight (aluminum frame minus thrust ring and hairpin barbs) = 0.912 lb

(b) Support frame.

Figure 4.- Continued.

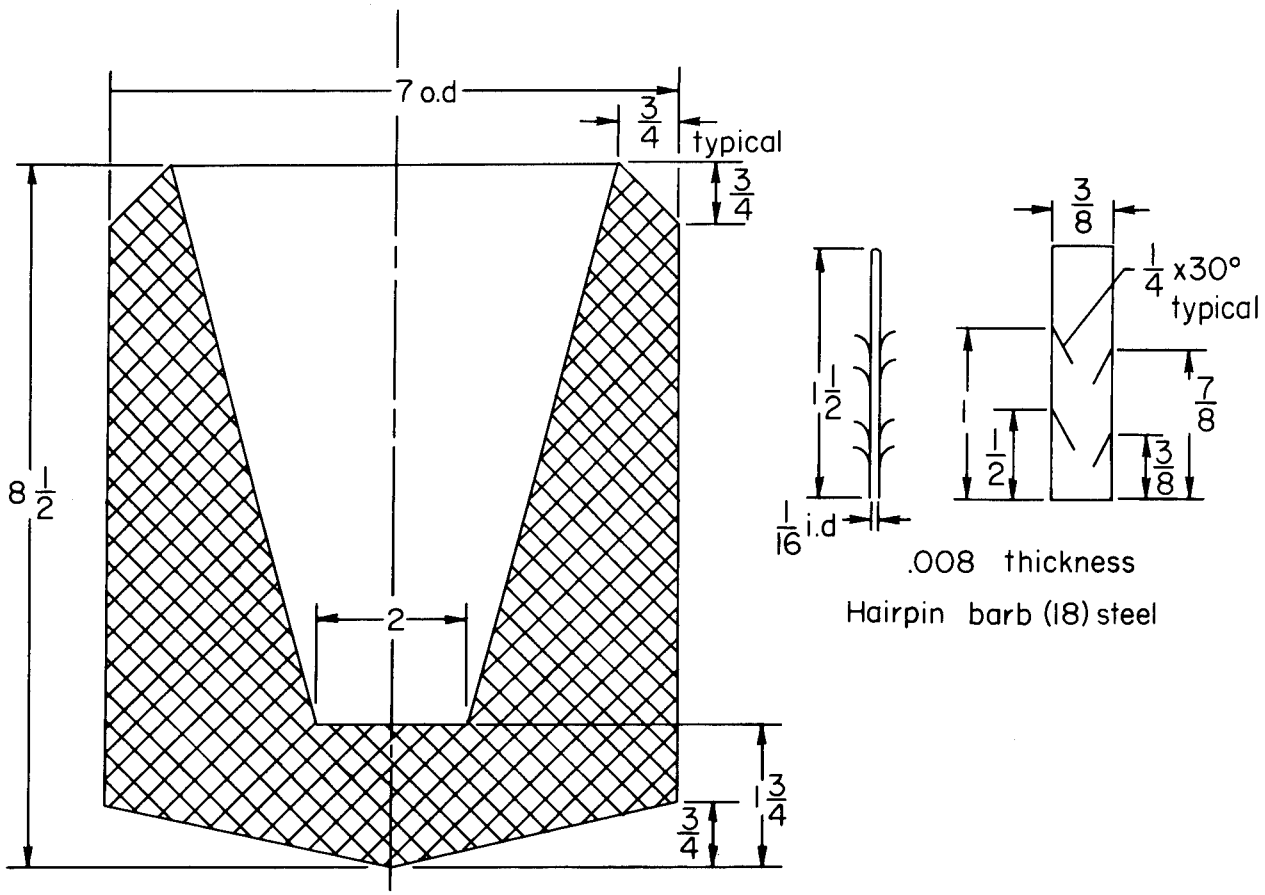

Material = polystyrene foam
Density = 1.8 lb/ft^3
Crushable height (foam) = 8.25 in.
Weight, (3 pads including 18 hairpin barbs) = 0.768 lb
Hairpin barbs (steel) (to hold foam on cutters) (6 per cutter) = 0.046 lb

(c) Foam gear pads.

Figure 4.- Concluded.

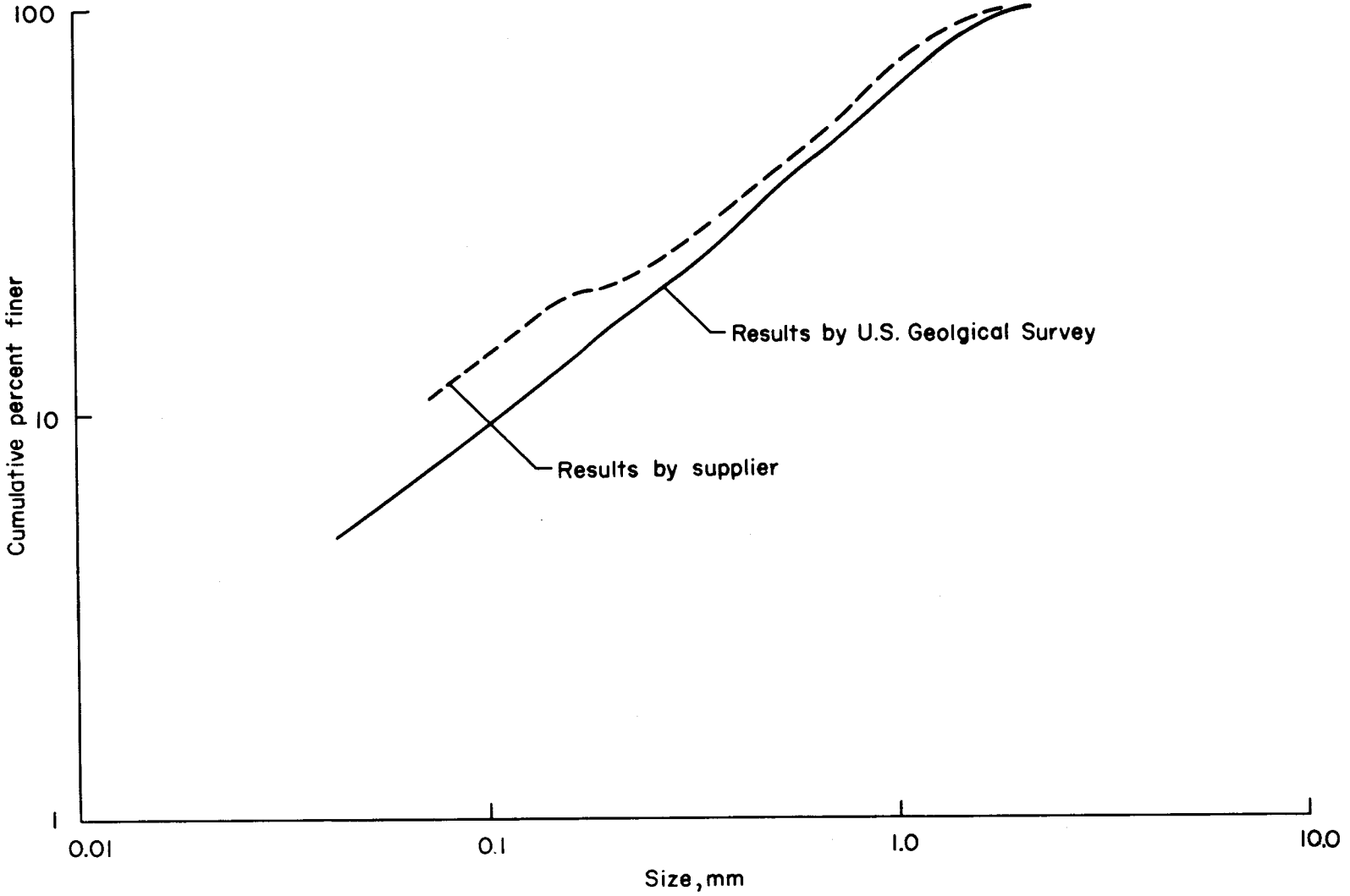

Figure 5.- Sieve results for crushed basalt.

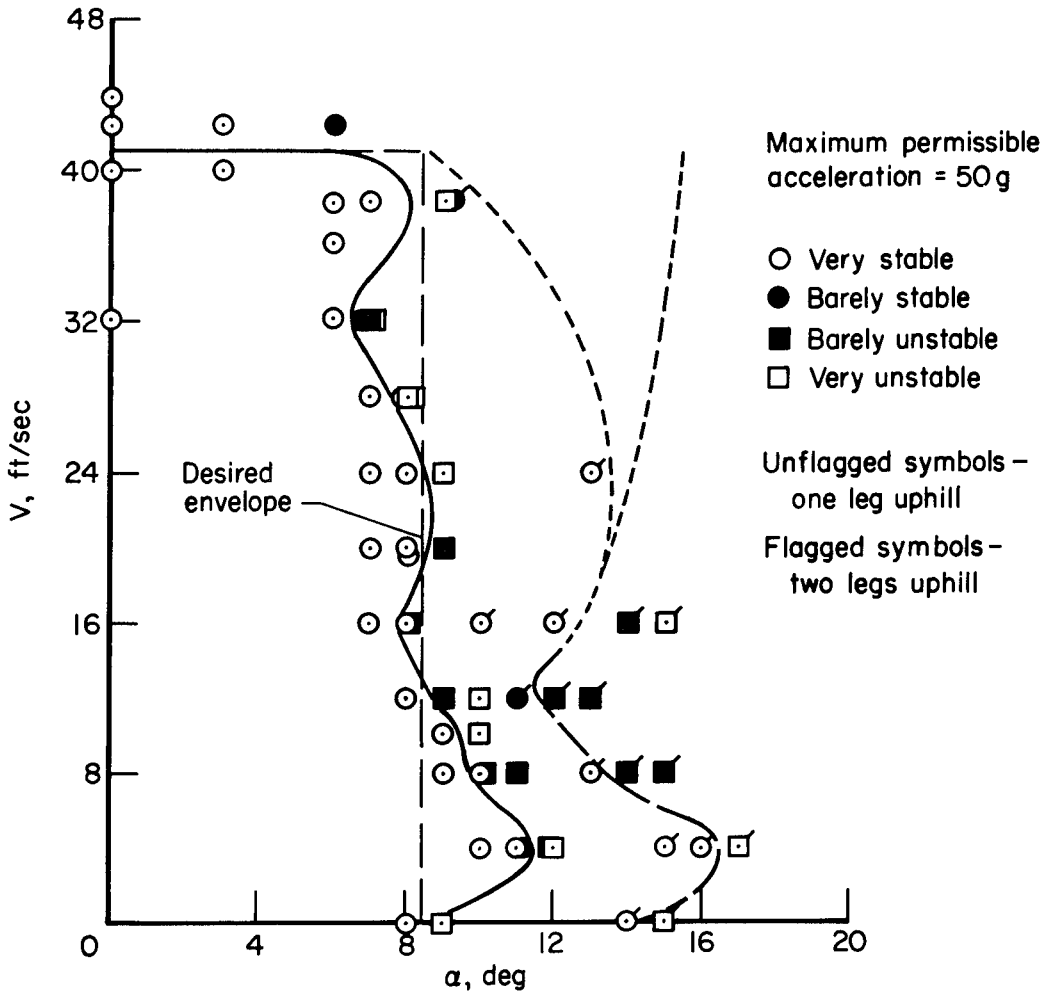

(a) Vertical impacts on crushed basalt.

Figure 6.- Energy absorption and tip-over stability for various impact velocities and ground slopes.

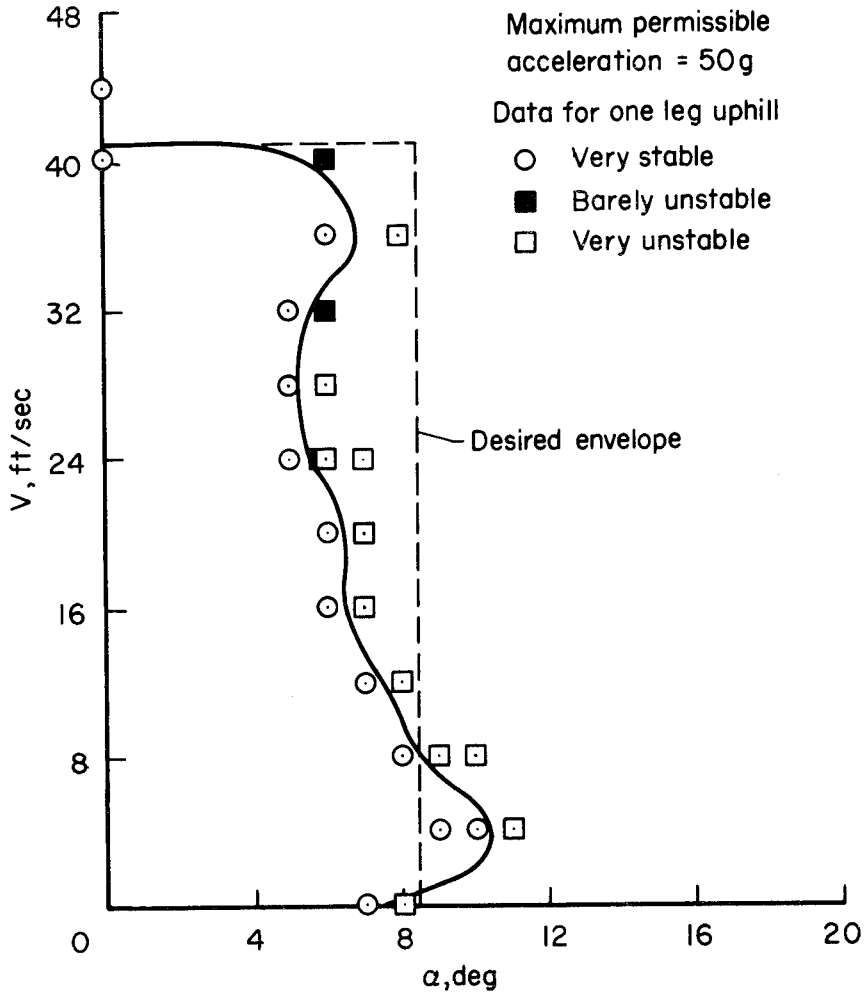

(b) Vertical impacts on steel.

Figure 6.- Continued.

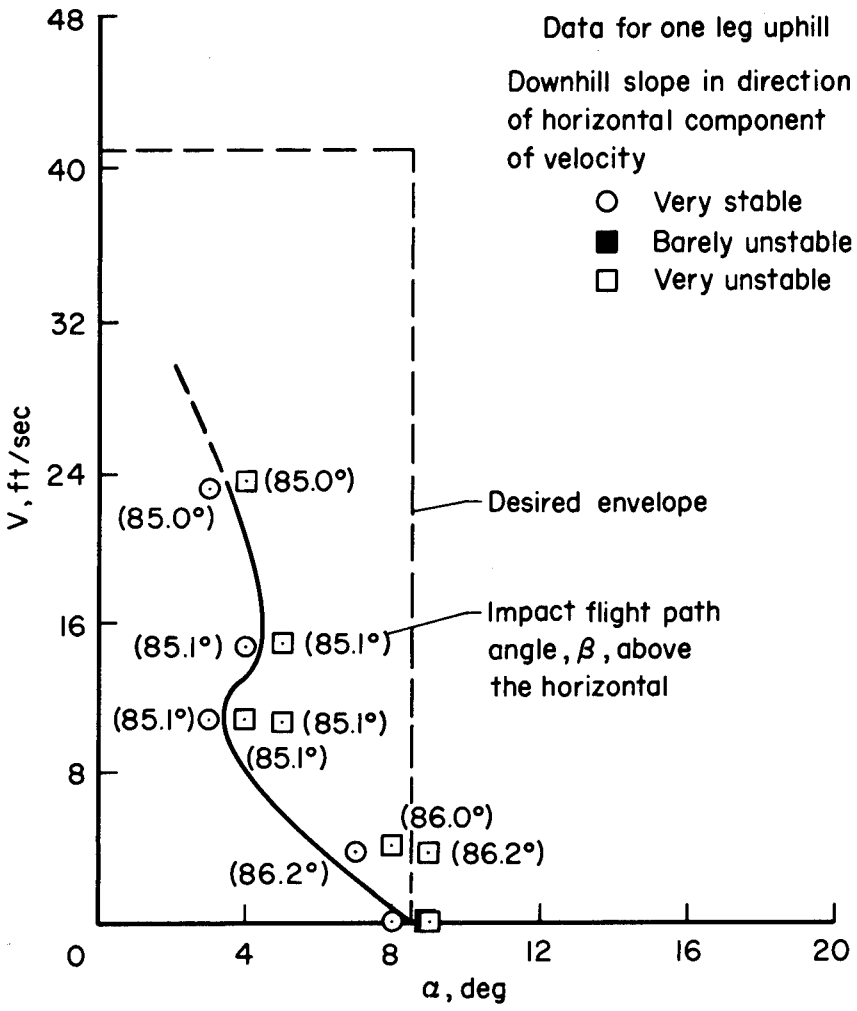

(c) Impacts on crushed basalt, β approximately 85°.

Figure 6.- Concluded.

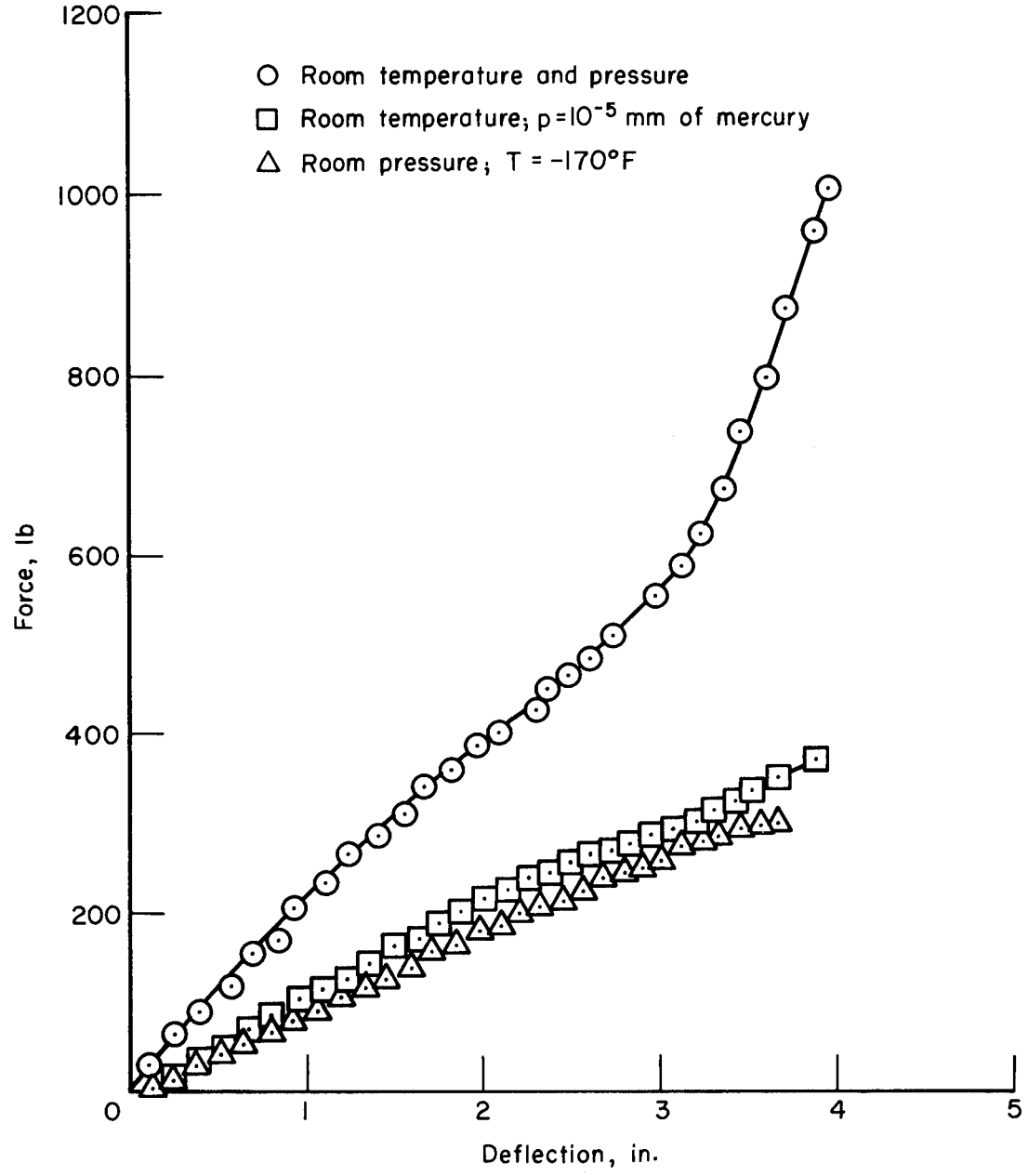

Figure 7.- Effect of vacuum and low temperature on crushing of solid foam sphere.

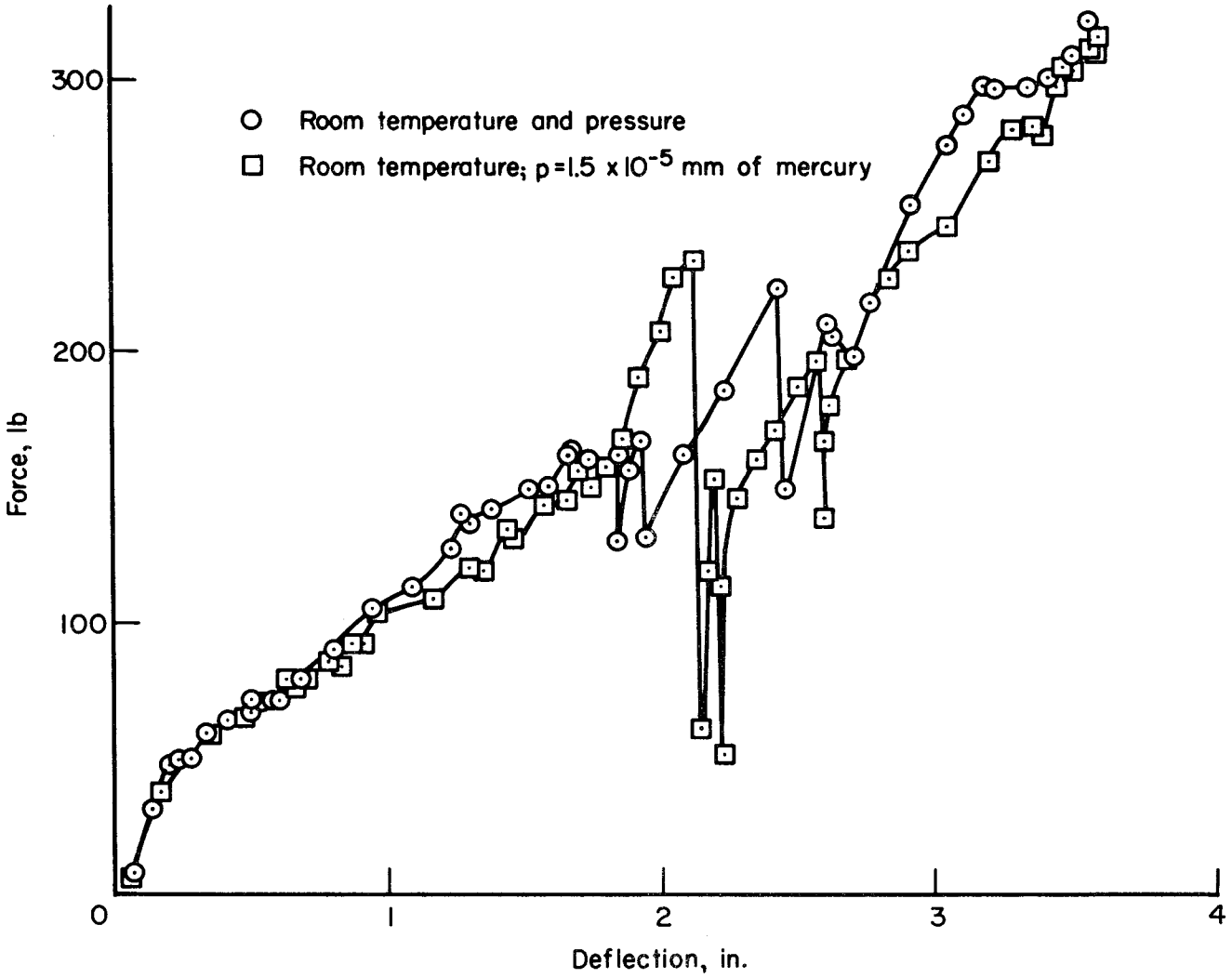

Figure 8.- Effect of vacuum on cutting of foam.

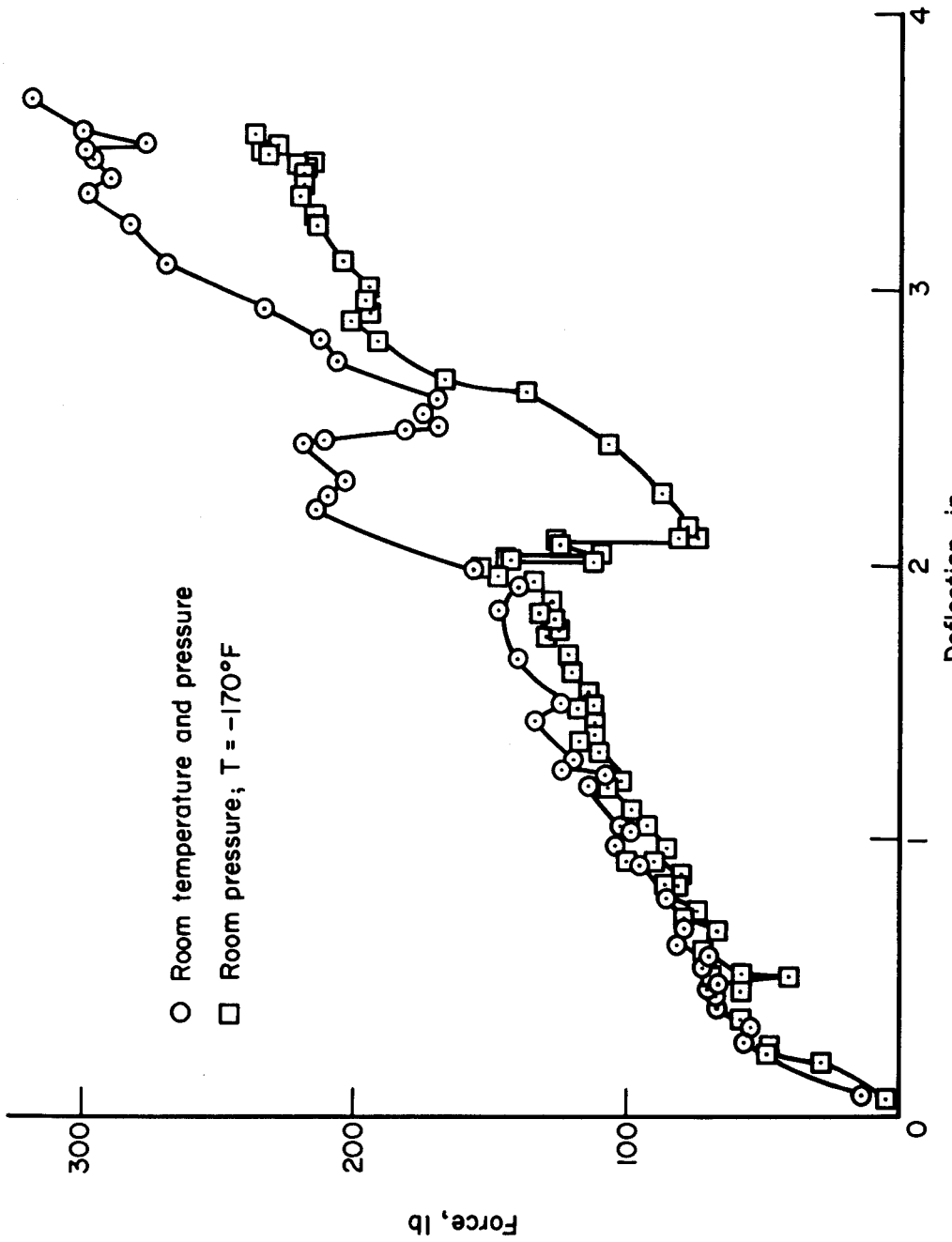

Figure 9.- Effect of low temperature on cutting of foam.

"The aeronautical and space activities of the United States shall be conducted so as to contribute . . . to the expansion of human knowledge of phenomena in the atmosphere and space. The Administration shall provide for the widest practicable and appropriate dissemination of information concerning its activities and the results thereof."

—NATIONAL AERONAUTICS AND SPACE ACT OF 1958

NASA SCIENTIFIC AND TECHNICAL PUBLICATIONS

TECHNICAL REPORTS: Scientific and technical information considered important, complete, and a lasting contribution to existing knowledge.

TECHNICAL NOTES: Information less broad in scope but nevertheless of importance as a contribution to existing knowledge.

TECHNICAL MEMORANDUMS: Information receiving limited distribution because of preliminary data, security classification, or other reasons.

CONTRACTOR REPORTS: Technical information generated in connection with a NASA contract or grant and released under NASA auspices.

TECHNICAL TRANSLATIONS: Information published in a foreign language considered to merit NASA distribution in English.

TECHNICAL REPRINTS: Information derived from NASA activities and initially published in the form of journal articles.

SPECIAL PUBLICATIONS: Information derived from or of value to NASA activities but not necessarily reporting the results of individual NASA-programmed scientific efforts. Publications include conference proceedings, monographs, data compilations, handbooks, sourcebooks, and special bibliographies.

Details on the availability of these publications may be obtained from:

SCIENTIFIC AND TECHNICAL INFORMATION DIVISION

NATIONAL AERONAUTICS AND SPACE ADMINISTRATION

Washington, D.C. 20546